ACS OMEGA

http://pubs.acs.org/journal/acsodf

Article

# A Novel Chemical−Electrochemical Hydrogen Production from Coal Slurry by a Two-Step Process: Oxidation of Coal by Ferric Ions and Electroreduction of Hydrogen Ions

Niyi Olukayode, Weijing Yang, Kang Xiang, Shenrong Ye, Zhigang Sun, Zhenfei Han, and Sheng Sui*

Cite This: *ACS Omega* 2022, 7, 7865−7873

Read Online

ACCESS | Metrics & More | Article Recommendations

**ABSTRACT:** Hydrogen production from the electrolysis of coal slurry is a promising approach under the condition of low voltage (0.8−1.2 V) and medium temperature. However, the rate of hydrogen production is slugged by poor anode kinetics, under an electrochemical condition that results from the collision of the coal particles with the anode surface. This paper reports a novel process that consists of two steps: the oxidation of the coal slurry by ferric ions(III) in a hydrothermal reactor at a temperature of 120−160 °C and the electro-oxidation of ferric ions(II) in the electrochemical cell to produce hydrogen. This technique circumvents the technical issues experienced in the conventional coal slurry electrolysis process by adopting a two-step process consisting of solid−liquid reactions instead of solid−solid reactions. This indirect oxidation process produced a current density of 120 mA/cm$^2$ at room temperature and a voltage of 1 V, which is higher than the values reported in the conventional processes. An investigation of the oxidation mechanism was carried out via scanning electron microscopy, Fourier-transform infrared spectroscopy and elemental analysis. The results obtained showed that the oxidation of coal by ferric ions occurs from the surface to the inner parts of the coal particles in a stepwise manner. It was also revealed that the ferric ions in the media increased the active interfaces both of the coal particles and of the anode electrode. This explains the high hydrogen production rate obtained from this process. This novel discovery can pave the way for the commercialization of coal slurry electrolysis.

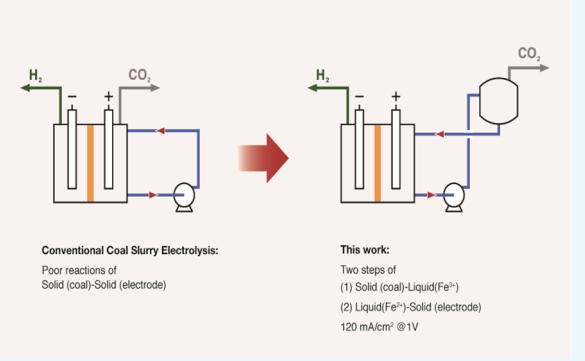


## 1. INTRODUCTION

The generation of energy from hydrogen has attracted enormous research interest because of its reliability, sustainability, and environmental safety. Hydrogen gas is an excellent energy carrier; it is clean and attractive for energy conversion and storage due to its high gravimetric energy density and relatively high heating value (39.05 W h/kg).[1] However, hydrogen gas does not occur freely in nature; it has to be produced from a wide range of sources such as coal, natural gas, and nuclear and renewable energy.[2] The commonly used methods for producing hydrogen gas include steam reforming, coal gasification, and water electrolysis. Steam reforming is nonrenewable and produces a high quantity of carbon monoxide.[3] Gasification of coal is another common method, but its end product consists of impurities. It requires a temperature as high as 800 °C;[4] the process is inefficient, and it leads to the emission of a large quantity of $CO_2$.[5] On the other hand, the water electrolysis method produces pure hydrogen, and it generates no greenhouse gases; however, the high energy consumption and the cost of this process hinder its widespread application.[6] Alternative methods have been deployed to reduce the high energy consumption associated with water electrolysis; one such method involves the electrolysis of carbon-rich sources such as coal, alcohol, and biomass.[7] The use of liquid carbon sources[8−11] and biochar[1,12] for carbon-assisted water electrolysis has been reported to be effective in reducing the energy consumption associated with the production of hydrogen during water electrolysis to a value as low as 0.5 V, and has improved pure hydrogen production. Low cost, easy accessibility of coal, and the relatively clean nature of the procedure have made the production of hydrogen through the electrolysis of coal a competitive and viable method for the future.

Hydrogen production by coal slurry electrolysis was pioneered by Coughlin and Farooque in 1979.[13−15] The process involves two half-reactions in an electrochemical cell in which coal is oxidized to carbon dioxide at the anode and

**Received:** November 30, 2021
**Accepted:** February 1, 2022
**Published:** February 23, 2022





https://doi.org/10.1021/acsomega.1c06759
*ACS Omega* 2022, 7, 7865−7873

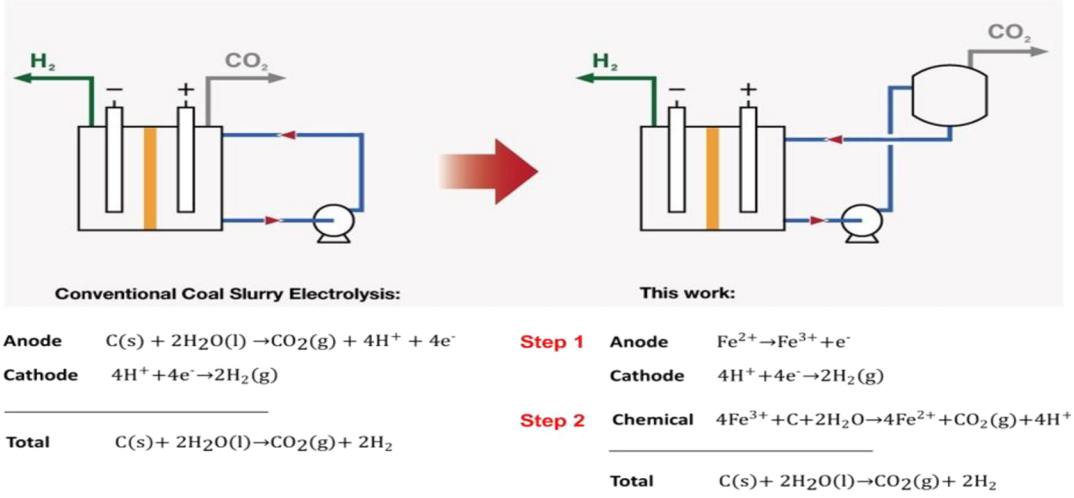


**Figure 1.** Schematic comparison between conventional coal electrochemical oxidation and the novel two-step process.

**Table 1. Industrial Analysis of Indonesia Coal, Xinjiang Coal, Mingjia Coal, and Yangquan Coal**

| | moisture (wt %) | ash (wt %) | volatile (wt %) | fixed carbon (wt %) | C (wt %) | H (wt %) | O (wt %) | N (wt %) | S (wt %) |
|---|---|---|---|---|---|---|---|---|---|
| Indonesia coal | 16.4 | 4.11 | 46.17 | 33.32 | 50 | 4.06 | 24.57 | 0.64 | 0.22 |
| Xinjiang coal | 13.25 | 4.05 | 29.79 | 52.91 | 65.43 | 3.76 | 12.17 | 0.63 | 0.71 |
| Mingjia coal | 3.11 | 4.38 | 34.16 | 58.35 | 75.75 | 4.67 | 11.01 | 0.85 | 0.23 |
| Yangquan coal | 0.90 | 20.99 | 7.56 | 70.55 | 71.40 | 2.48 | 1.09 | 1.00 | 2.14 |

hydrogen is produced at the cathode. The redox reactions are expressed as follows:

$$C(s) + 2H_2O(l) \rightarrow CO_2(g) + 4H^+ + 4e^- \quad (1)$$

$$4H^+ + 4e^- \rightarrow 2H_2(g) \quad (2)$$

Reactions (1) and (2) take place at the anode and cathode, respectively. The overall reaction in the electrochemical gasification of coal is given by

$$C(s) + 2H_2O(l) \rightarrow CO_2(g) + 2H_2(g) \quad (3)$$

In terms of energy consumption, the electrolysis of coal is preferred to water electrolysis; this is because 56.7 kcal of electrical energy and a reversible potential of 1.23 V are required to produce 1 mol of hydrogen in water electrolysis, whereas coal electrolysis only requires 9.5 kcal and 0.21 V, respectively.[16,17] This is achieved because the oxygen evolution reaction, which has high overpotential, is replaced with coal oxidation at the anode.[18] Despite this advantage, the production of hydrogen through the electrolysis of coal slurry is retarded by poor reaction kinetics, low current density, and low degradation degree of coal.[4,18] This makes the process uneconomical and the technology unavailable for commercialization. Therefore, to keep pace with the increase in the demand for pure hydrogen, the electrolysis of coal slurry requires to be made more efficient.

To this end, many researchers have investigated and developed novel electrocatalysts and electrode structures.[17,19−25] Effects of phenomena such as temperature[26−28] and coal morphology[29] have also been explored; increasing the temperature was found to improve the kinetics of coal electro-oxidation reaction, coal conversion rate, and $CO_2$/coal Faradaic efficiency. The presence of inherent minerals $Fe^{2+}$ and $Fe^{3+}$ in coal has also been found to have a significant effect on the electro-oxidation process, hydrogen evolution reaction, and coal degradation reaction.[30−32] The high current density produced during the electrolysis of coal slurries is attributed to the presence of $Fe^{2+}$ and $Fe^{3+}$ ions in the coal.[18,21] The mechanism involves the oxidation of coal slurry at the platinum electrode by $Fe^{3+}$ ions, which is reduced to $Fe^{2+}$ ions; consequently, at the anode, the $Fe^{2+}$ ion is re-oxidized to the $Fe^{3+}$ ion.[32] This anodic oxidation is responsible for the current produced during coal-assisted water electrolysis.[31,33] The process can be summarized by the following two reactions at the anode

$$4Fe^{2+} \rightarrow 4Fe^{3+} + 4e^- \quad (4)$$

$$4Fe^{3+} + C + 2H_2O \rightarrow 4Fe^{2+} + CO_2(g) + 4H^+ \quad (5)$$

Even with the increase in the hydrogen production capacity of the coal slurry electrolysis through the improvements in the electrodes, electrocatalysts, and coal types and particle sizes, there are still concerns about productivity because of the solid−solid phase interface created by the coal particles and the electrode.[34,35] This paper seeks to overcome these challenges by introducing a novel process that involves an indirect oxidation mechanism of ferric ions, as shown in Figure 1. This technique involved dividing the conventional solid−solid reaction into two solid−liquid reactions, thereby avoiding the existing technical issues and increasing the hydrogen production rate.

## 2. MATERIALS AND METHODS

**2.1. Selection of Coal Samples and Preparation of the Slurry.** Four coal samples were used for the present investigation. They are Indonesia coal, Xinjiang coal, Mingjia coal, and Yangquan coal (Table 1). Yangquan coal (anthracite coal) has the highest rank, while Indonesia coal (lignite coal) has the lowest rank of the coal samples. The coal samples were crushed to a particle size of 100−125 $\mu$m, and the coal slurry



https://doi.org/10.1021/acsomega.1c06759
ACS Omega 2022, 7, 7865−7873

was made with ferric sulfate [$Fe_2(SO_4)_3$], sulfuric acid ($H_2SO_4$), and deionized water. The coal slurry comprises 1 mol/L $Fe^{3+}$, 1 mol/L $H_2SO_4$, and 20 g/L raw coal.

**2.2. Electrode Preparation.** The platinum black electrodes were prepared by the electrodeposition method. The platinum sheet was cut into 1 × 1 $cm^2$ and was polished with fine sandpaper. NaOH solution (1 mol/L) was used to clean the grease on the surface of the platinum sheets at 65 °C for 30 min. After washing several times with deionized water, a clean platinum electrode was obtained. In this experiment, a platinum black electrode was prepared by reducing chloroplatinic acid ($H_2PtCl_6$) with an additive. 1000 mg of $H_2PtCl_6$ and 5.7 mg of $(CH_3COO)_2Pb$ were added to a beaker and ultrasonically stirred for 15 min. After the dissolution of the solid particles, a platinizing solution was obtained. Two pieces of the cleaned platinum sheets, one as working electrode and the other one as counter electrode, were immersed in the solution. Thereafter, a constant current of 30 mA/$cm^2$ was applied for 10 min. Then, the two electrodes were switched and the process was repeated. After three cycles, a layer of black velvet was deposited on the platinum sheet and the electrochemical activity of the electrode was observed.

**2.3. Experimental Setup of the Electrochemical Cell.** The electrochemical cell is made of Teflon, and it consists of Nafion 1135, a proton exchange membrane which separate the anode and the cathode chambers. The solution in the cathode chamber is 1 mol/L $H_2SO_4$, while the anode contains the coal slurry oxidized by the ferric ions in the hydrothermal reactor. A constant voltage of 1 V was maintained throughout the process. However, the current was observed to decrease with time due to the reduction in the concentration of $Fe^{2+}$ upon its oxidation in the anode. The indicators of the performance of the electrolytic process are the initial current density and electric quantity. Initial current density is the current density at the beginning of electrolysis, and electric quantity is the accumulated electric quantity when electrolysis ends. The former reflects the rate of hydrogen production, and the latter reveals the quantity of hydrogen which can be collected.

**2.4. Experimental Procedure.** Lignite and sub-bituminous coals possess inherent high moisture and oxygen content and low calorific heating value; this necessitates the conditioning of these coals under hydrothermal conditions to alter the physical, chemical, and rheological properties of the coal.[36] The thermochemical process produces a fairly cleaned and thermally upgraded coal product that would not reabsorb moisture even when placed in a water medium at high pressure.[36] This experiment was conducted in two steps; in the first step, the coal slurry was heated in a hydrothermal reactor and oxidized by $Fe^{3+}$ ions for 3 h within the temperature range of 120−160 °C. The hydrothermal reactor is made up of stainless steel which houses a beaker. The volume of the reactor is 350 mL, and the permitted highest temperature in the reactor is 180 °C. The second step involves pumping the resulting solution into the anode chamber of an electrochemical cell, and subsequent electrolysis at a constant voltage of 1 V to collect pure hydrogen. The ferric ions in the solution, which can be used repeatedly, accelerated this process by increasing the frequency of collision and the area of contact between the coal particles and the anode. This phenomenon is hardly achieved between coal particles and electrodes during the conventional electrolysis of coal slurry.

## 2.5. RESULTS AND DISCUSSION

**2.6. Elemental Analysis.** The elemental analysis of Xinjiang coal was carried out after two different cycles of the process (raw coal, coal after 4 cycles, and coal after 13 cycles). Table 2 shows the weight percentage of C, H, N, S, and O in the dry and ash-free Xinjiang coal. The atom ratios of carbon to hydrogen of Xinjiang coal in three different stages of the process are 1.45, 1.52, and 1.76, respectively. There is an observed increase in the C/H ratio, and this suggests that the coal was made from more unsaturated groups during the oxidation process. This is attributed to the presence of more double bonds, triple bonds, or other unsaturated functional groups after several cycles. Similarly, the atom ratio of carbon to oxygen was found to be 7.17, 5.64, and 8.27, respectively. Initially, there was a recorded decrease in the C/O ratio in the first four cycles; this happened because more oxygen atoms from water molecules were added into the coal structure during this stage. However, after 13 cycles, the coal has the highest C/O ratio; this occurs because matters with low C/O such as $CO_2$ were released from the coal slurry. The $CO_2$ released during this process accounts for the production of carbon dioxide in the hydrothermal reactor. The chemical reaction between coal, $Fe^{3+}$ and water breaks water molecules into hydrogen and oxygen atoms. While the hydrogen atoms are released into the solution as ions, oxygen atoms are embedded into coal. This action leads to the formation of many partial oxidation structures such as C−O−C, C═O, and C−O−OH. These oxidised structures have poor thermal stability, and the eventual thermal decomposition of these structures leads to the production of $CO_2$. As a result of the incomplete thermal decomposition of the partial oxidised structures, the quantity of $CO_2$ obtained from this process was less than the expected value, which according to Farooque and Coughlin[15] should have a volume ratio ($CO_2$ = $H_2$) of 1/2.

**Table 2. Elemental Analysis of Xinjiang Coal after Two Different Cycles of the Process**

| | C (wt %) | H (wt %) | N (wt %) | S (wt %) | O (wt %) | C/H (at) | C/O (at) |
|---|---|---|---|---|---|---|---|
| raw coal | 79.12 | 4.55 | 0.76 | 0.86 | 14.71 | 1.45 | 7.17 |
| coal in 4 cycles | 76.47 | 4.18 | 0.67 | 0.61 | 18.07 | 1.52 | 5.64 |
| coal in 13 cycles | 81.53 | 3.86 | 0.77 | 0.69 | 13.15 | 1.76 | 8.27 |

**2.7. Scanning Electron Microscopy Analysis.** Figure 2 reveals the structure of the raw and processed coal samples. It can be observed that the particles of raw coal have sharp edges and corners. However, after oxidation, they became elliptical with smooth velvet surfaces. The reason for this change in appearance is attributed to the erosion of the surface of the coal particles as a result of the oxidation . Thomas et al.[37] revealed that as the coal surface becomes rougher, the active sites in the particles are exposed. This enhances a deeper interaction between the coal particles and the ferric ions.

**2.8. Fourier Transform Infrared Spectra Analysis.** The Fourier transform infrared spectra of coal samples were used to observe the structural changes of the coal samples. The quantitative changes in the structures before and after electrolysis were investigated by comparing the intensity of each peak in the same spectrum. The variation in the intensity of the signals obtained connotes different molecular reactions



https://doi.org/10.1021/acsomega.1c06759
ACS Omega 2022, 7, 7865−7873

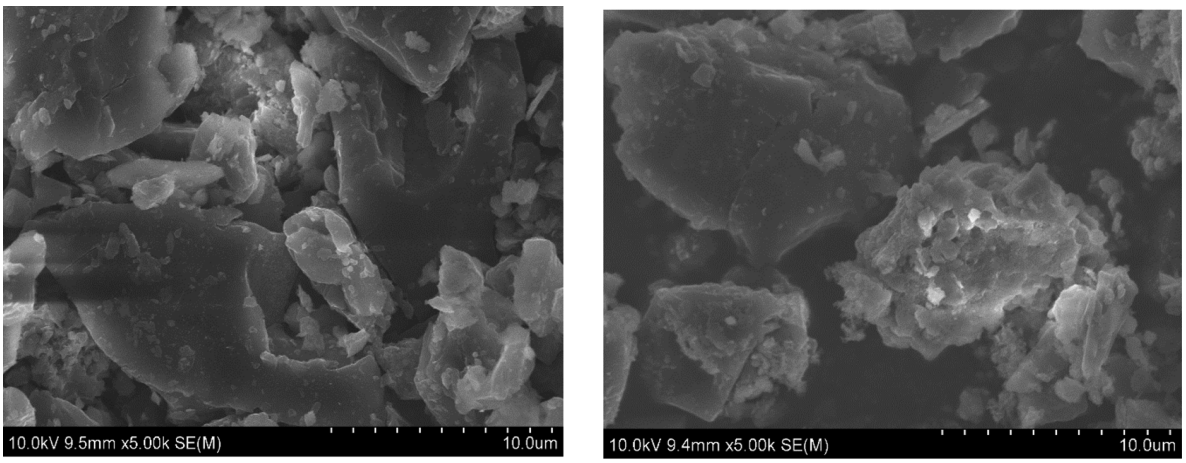


**Figure 2.** Scanning electron microscopy images of Yangquan coal. (a) Raw ; (b) processed after 4 cycles (160 °C, 2 h).

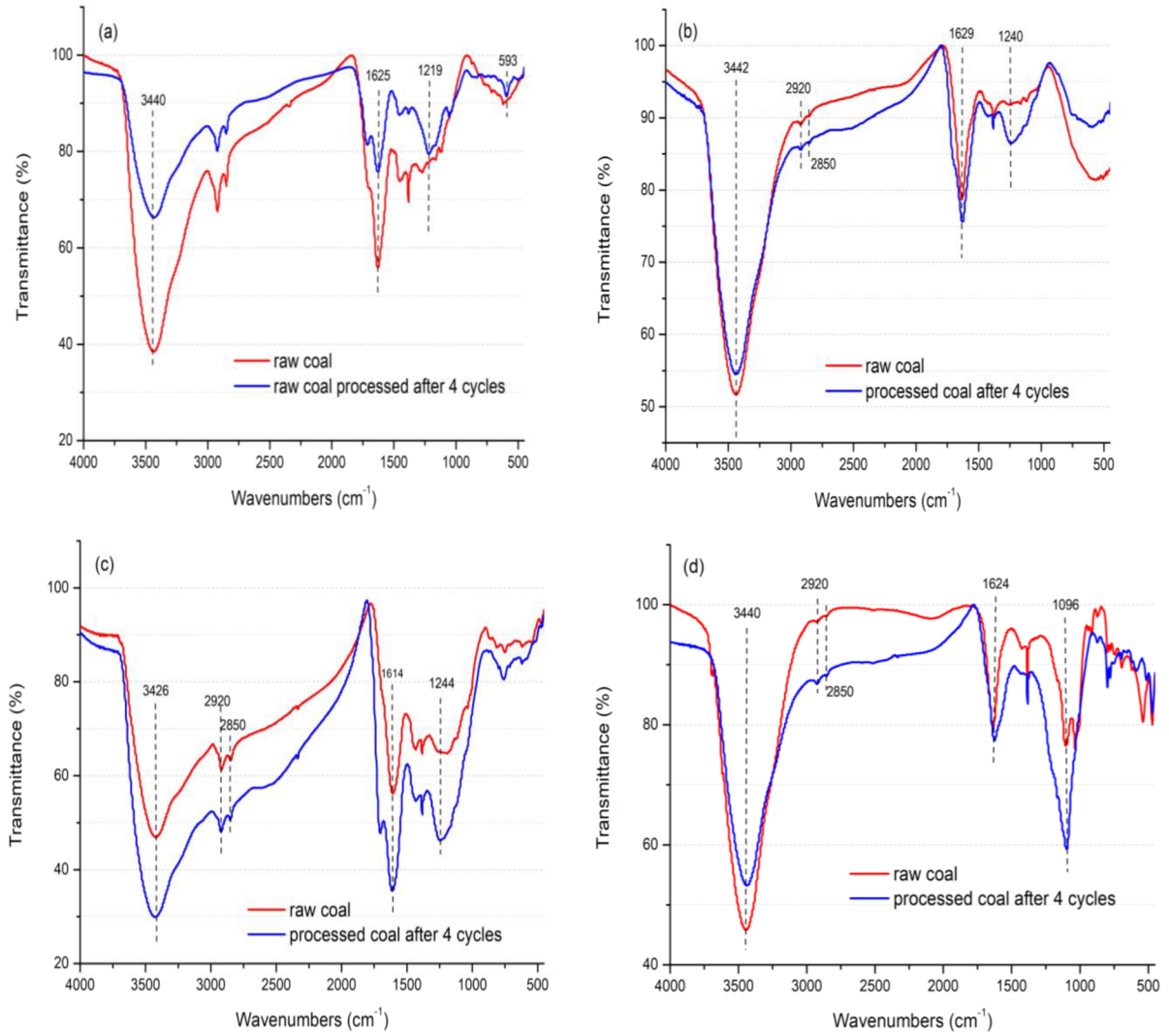


**Figure 3.** Fourier transform infrared spectra of coal samples before and after four cycles. (a) Indonesia coal; (b) Xinjiang coal; (c) Mingjia coal; and (d) Yangquan coal (160 °C, 2 h).

in the specimen. According to Miura et al.,[38] the broad peak near 3440 $cm^{-1}$ is associated with the stretching vibration of the −OH or O−H bond. On the other hand, the absorption peaks at 2920 and 2850 $cm^{-1}$ are attributed to the stretching vibration of $-CH_3-$ and $-CH_2-$ bonds, respectively. The peaks near 1625, 1240, and 1100 $cm^{-1}$ represent the vibration



https://doi.org/10.1021/acsomega.1c06759
ACS Omega 2022, 7, 7865−7873

of the unsaturated double bond relating to C═C, C═O, and C−O respectively.[39,40] When compared to the spectrum of their raw coals, the ratios of peak heights (1625 to 3440 $cm^{-1}$) increased significantly in the processed coal after 4 cycles, as shown in Figure 3b, d. This indicates an increase in the unsaturated structures of C═C and C═O in Xinjian coal and Yangquan coal during the oxidation process. The C−O group is also expected to increase. On the contrary, after four cycles of electrolysis, the ratios of the peak height shown in Figure 3a, c at this spectrum did not have a significant increase when compared to the spectrum of the raw Indonesia coal and Mingjia coal. A significant difference is that the peak height ratios at 2920 and 2850 $cm^{-1}$ shown in Figure 3a, c are higher than those shown in Figure 3b, d. The relative decrease in (a) and (c) can be attributed to the presence of more aliphatic compounds in Indonesia and Mingjia coal. During the breaking down of carbon chains in the aliphatic compounds, more oxidised products were released into the solution. However, this may not happen in aromatic compounds because of their stability. The total organic carbon (TOC) in the electrolysed solution after four cycles is presented as follows.

As shown in Table 3, the electrolysed solutions of Indonesia and Mingjia coals have a higher TOC than those of Xinjiang and Yangquan coals after four cycles of electrolysis. Although Indonesia coal has the highest TOC, it shows the least increase in oxidised structures, as revealed in Figure 3a. This confirms the possibility that some oxidised products are dissolved in the electrolysed solution after the breaking of carbon chains.

**Table 3. Total Organic Carbon (TOC) in the Electrolysed Solution after Four Cycles of Electrolysis**

| | Indonesia coal | Xinjiang coal | Mingjia coal | Yangquan coal |
|---|---|---|---|---|
| TOC, mg/L | 950.4 | 258.0 | 348.1 | 139.1 |

**2.9. Effect of Oxidation Time on Hydrothermal Reaction.** The kinetics of electrochemical oxidation is slow in a conventional water-splitting electrolytic system. However, it has proven to be rapid and efficient in hydrothermal electrolysis.[41] In the hydrothermal reactor, liquid-phase oxidation of coal occurs in the presence of oxygen. The kinetics of this electrochemical reaction is deduced from the current density. In the hydrothermal reactor, the oxidation reaction is stopped after the first 3 h. The variation of initial current density with time is then observed.

After the end of the first 3 h, the oxidation reaction rate increased slowly . According to Figure 4, the corresponding initial current density obtained at this point is 95 $mA/cm^2$. Beyond this time, there was no significant increase in the initial current density. During the electrolysis, electro-oxidation of iron ions occurred, the effect of which can be understood by determining the concentration of $Fe^{2+}$ and $Fe^{3+}$ ions in the coal slurry. This is done by investigating the initial current density at different concentrations of $Fe^{2+}$ ions. Figure 5 reveals that the higher the concentration of $Fe^{2+}$, the higher is the current density. This increase in current density is attributed to the presence of iron ions in the solution; this is consistent with many research findings.[21] Figure 5 also shows that the concentration of $Fe^{2+}$ corresponding to the electrolytic initial current density of 95 $mA/cm^2$ is 0.4 mol/L. This implies that the concentration of $Fe^{2+}$ after the first 3 h is about 0.4 mol/L,

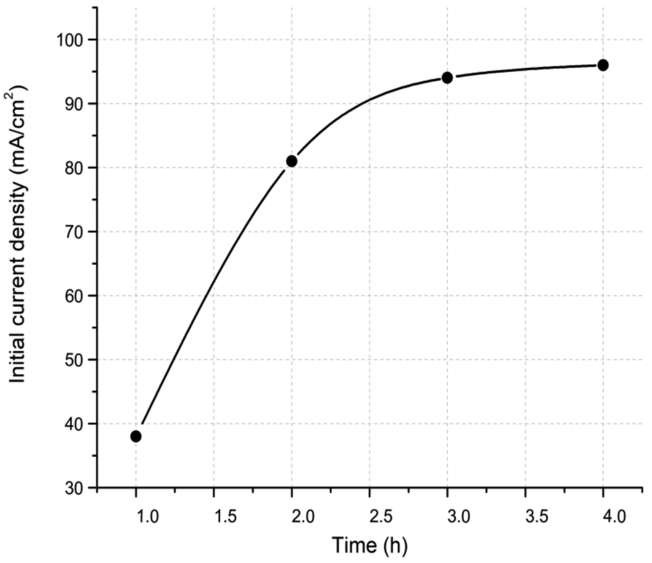


**Figure 4.** Effect of oxidation time on initial current density (Indonesia coal at 140 °C).

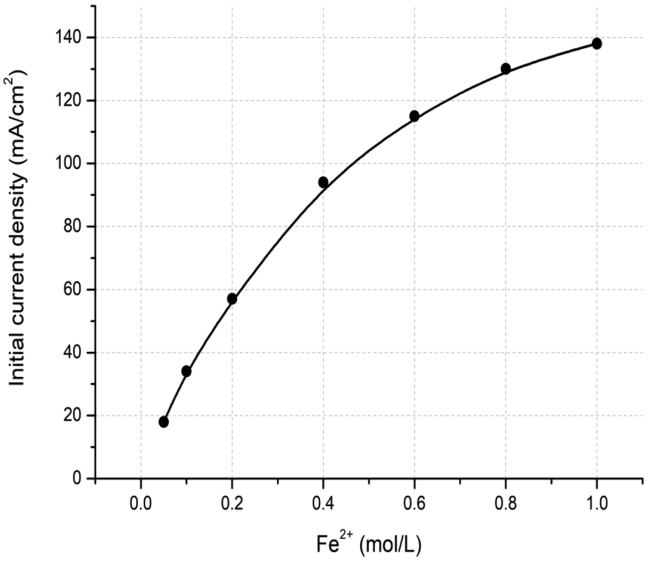


**Figure 5.** Initial current density vs $Fe^{2+}$ concentrations (1 mol/L $H_2SO_4$ and 1 V).

thereby indicating the presence of a large quantity of $Fe^{3+}$ ions in the coal slurry. Also, it confirms the regeneration of $Fe^{3+}$ after electrolysis.

**2.10. Effect of Oxidation Temperature on Hydrothermal Reaction.** An increase in temperature has been proven to accelerate the slow reaction kinetics by reducing the activation energy during electrolysis.[26−28,42,43] Therefore, the reaction temperature is expected to have a significant effect on the hydrothermal reaction. Jia et al.[35] supported this assertion whenthey posited that the relationship between temperature and current density follows the Arrhenius equation. Figure 6 shows the variation of initial current density with temperature. The red line shown in the figure is a fitting curve whose form is referenced to the Arrhenius formula. The fitting curve equation for the curve is given below.

$$I = 983915\exp\left(\frac{-3906}{T}\right) \quad (6)$$



https://doi.org/10.1021/acsomega.1c06759
ACS Omega 2022, 7, 7865−7873

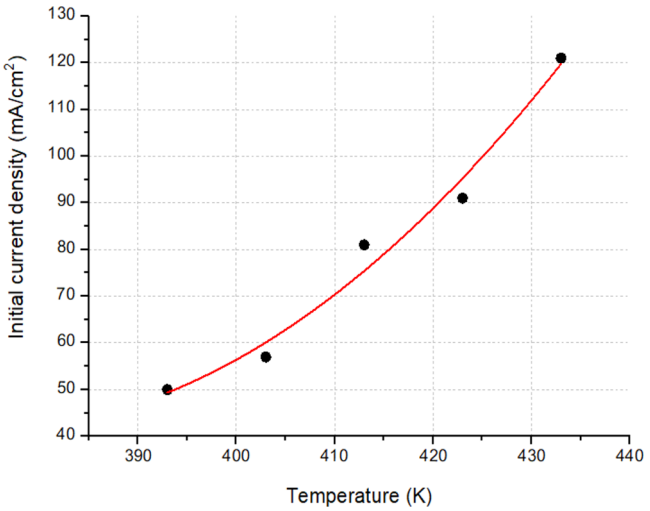


**Figure 6.** Effect of oxidation temperature on initial current density (Indonesia coal, reaction time 2 h).

where $I$ (mA/cm$^2$) is the initial current density and $T$ (K) is the oxidation temperature. Using the obtained curve fitting equation, the initial current density of electrolysis is estimated at 177 and 255 mA/cm$^2$ at a temperature of 180 and 200 °C, respectively.

**2.11. Effect of Coal Properties on Initial Current Density.** Coals have varying properties depending on their type, composition, thermal reactivity, textural difference, gas adsorption characteristics, and functional groups, etc. These properties imposes different effects on their electrochemistry. The effect of coal types (Indonesia coal, Xinjiang coal, Mingjia coal, and Yangquan coal), activated carbon, and graphite on initial current density was investigated and plotted as shown in Figure 7.

Figure 7 shows that Indonesia coal has the highest initial current density and graphite has the lowest one. The coals have a much higher initial current density than pure carbon matters (activated carbon and graphite). A keen observation of the four types of coal reveals a decrease in the initial current density from Indonesia coal to Mingjia coal. This suggests that the lower the carbonization degree of coal, the higher is the initial current density. Activated carbon and graphite are difficult to be oxidized by $Fe^{3+}$. It can be inferred that the oxidation sites in coal are mainly functional groups or aliphatic carbon attached to the core of coal, which is composed many of aromatic rings. Apart from this, a loose structure of coal or pure carbon matter makes it easy to oxidize. Table 4 gives details of the components of some coals and graphite. The table 4 shows that Indonesia coal, which produces the highest electrolytic current density, has the highest volatile matter and the lowest fixed carbon. Apart from this, Indonesia coal has the highest water content. The presence of water in coal increases its porosity, which in turn increases the specific surface area for oxidation. The atom ratio of carbon to hydrogen in Indonesia coal, Xinjiang coal, Mingjia coal, and Yangquan coal is 1.03, 1.45, 1.35, and 2.40, respectively. Also, the atom ratio of carbon and oxygen in Xinjiang coal, Mingjia coal, and Yangquan coal is 2.71, 7.17, 9.17, and 87.34, respectively. According to table 4, Yangquan coal has the highest ratio of C/H and C/O and a much lower electrolytic current density than Xinjiang coal and Mingjia coal. It is not a coincidence that Xinjiang coal and Mingjia coal have relatively close ratios of C/H and C/O and at the same time produce close values of electrolytic current density. This indicates that the presence of more hydrogen or oxygen atoms rather than those of carbon atoms in the coal slurry favors the oxidation of coal by ferric ions.

**2.12. Effect of Coal Slurry Compositions on Current Density and Electric Quantity.** To study the electrochemical kinetics of coal slurry electrolysis, the Tafel plot plays a crucial role. It is employed to represent the relationship between the overpotential and the logarithm of current density.[48] Current density is defined the charge per unit time flowing through a unit area of a cross section.[49] The current density is measured by a current measuring instrument placed external to the electrochemical cell, and the value obtained is actually the net current, which is a measure of the difference between the forward and reverse current on the electrode.[44] At equilibrium conditions, the rate at which the reactants are transformed into products and products are regenerated as reactants is called exchange current density.[45] This current density measures the electrode's readiness to proceed with the electrochemical reaction,[44] reflects the intrinsic rate of heat

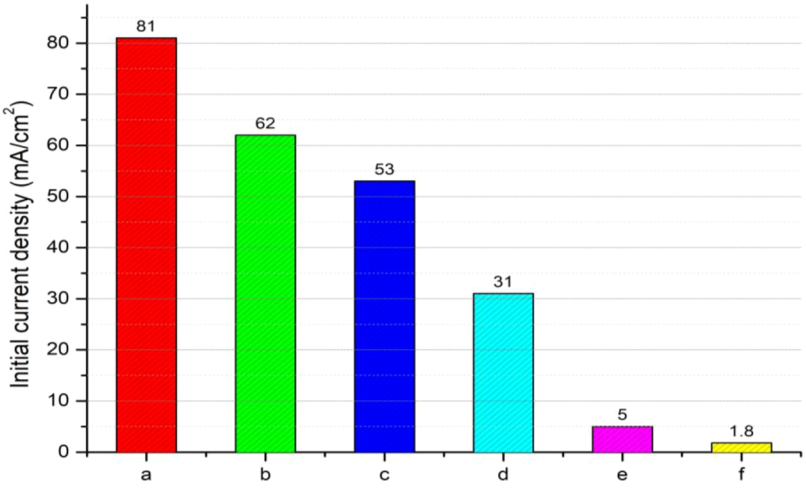


**Figure 7.** Effect of different coals, activated carbon, and graphite on initial current density (140 °C, 2 h). (a) Indonesia coal; (b) Xinjiang coal; (c) Mingjia coal; (d) Yangquan coal; (e) activated carbon; and (f) graphite.



https://doi.org/10.1021/acsomega.1c06759
ACS Omega 2022, 7, 7865−7873

Table 4. Components of Indonesia Coal, Xinjiang Coal, Mingjia Coal, Yangquan Coal and Graphite

| | water content (wt %) | ash content (wt %) | volatile matter (wt %) | fixed carbon (wt %) | C (wt %) | H (wt %) | O (wt %) | N (wt %) | S (wt %) |
|---|---|---|---|---|---|---|---|---|---|
| Indonesia coal | 16.4 | 4.11 | 46.17 | 33.32 | 50 | 4.06 | 24.57 | 0.64 | 0.22 |
| Xinjiang coal | 13.25 | 4.05 | 29.79 | 52.91 | 65.43 | 3.76 | 12.17 | 0.63 | 0.71 |
| Mingjia coal | 3.11 | 4.38 | 34.16 | 58.35 | 75.75 | 4.67 | 11.01 | 0.85 | 0.23 |
| Yangquan coal | 0.9 | 20.99 | 7.56 | 70.55 | 71.4 | 2.48 | 1.09 | 1 | 2.14 |
| graphite | | | | | 99.85 | | | | |

transfer between an electroactive specie and electrode, and provides insights into their structure and bonding.[46] The initial current density governs the rate at which an electrochemical reaction occurs on the surface of an electrode.[44] Therefore, this parameter is considered important for the characterization of the electrocatalytic activity and performance in the electrode[46,47] and in the determination of the rate of hydrogen production.

To investigate the effect of coal particles in the slurry on current density and electric quantity, 0.5 mol/L $Fe^{2+}$ solution was prepared with 1 mol/L $H_2SO_4$ solution and $FeSO_4$ solid and compared. The coal slurry has a coal mass concentration of 20 g/L. Figure 8 indicates that the suspension of coal

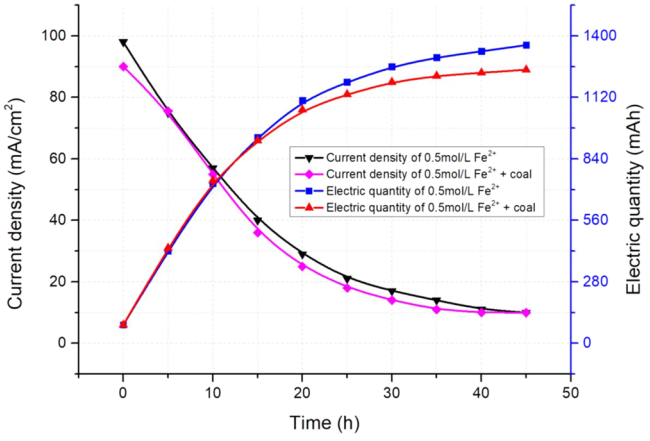


Figure 8. Effect of coal particles in slurry on current density and electric quantity.

particles in the solution can reduce the performance of electrolysis to some extent when compared with the 0.5 mol/L $Fe^{2+}$ solution after 12 h. Before that, the coal particles contribute small current. A possible reason is that the coal particles disturb the charge transfer in the solution or occupy the activated sites on the electrode. It is also possible that the coal particles diminish the concentration of $Fe^{2+}$ by adsorbing some ferric ions. It can be interpreted that the conventional coal slurry electrolysis shows low performance due to the dual effects of coal particles.

Figure 9 reveals that the current density decreases with time during the electrolysis. The current density experienced a sharp decline in the first 10 h. It was observed that after 35 h of electrolysis, the current tends to zero. This means that the current resulting from the transfer of electrons between coal particles and the anode is negligible. This is because nearly all the $Fe^{2+}$ ions have been oxidized to $Fe^{3+}$ ions at that time.

**2.13. Explanation of the Oxidation Mechanism of Ferric Ions.** The possible oxidation mechanism of ferric ions for coal gasification is explained as follows. During electrolysis, hydrogen is generated from the reduction of $H^+$ at the cathode;

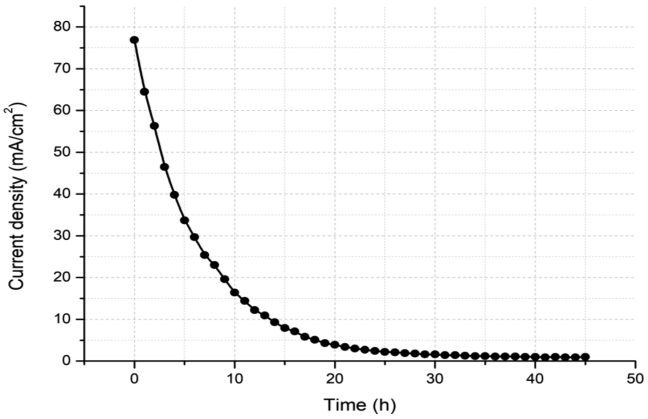


Figure 9. Current density decreases with the time of electrolysis of Xinjiang coal in the second cycle. (160 °C, 2 h).

the main reaction at the anode is the oxidation of $Fe^{2+}$. In the process of hydrothermal reaction, oxidation occurs on the active sites of the surface of coal particles or in the inner walls of the pores in coal particles. The oxidation between coal particles and ferric ions happens on the functional groups or aliphatic carbon attached to the core of the coal, which is composed of many aromatic rings. The products of oxidation are mainly organic matters which have been oxidized partially by ferric ions, such as aldehyde, organic acid, and ester. In this process, a large number of oxygen atoms from water molecules are added to the structure of coal. Carbon dioxide comes from the thermal decomposition of the products of the partial oxidation process. Meanwhile, the masses of organic matter are dissolved in the solution.

## 3. CONCLUSIONS

The novel cyclic hydrogen production has a higher reaction rate than that of conventional electrolysis of coal slurry. The initial current density in the novel process is 120 mA/cm$^2$, while that of conventional electrolysis of coal slurry is usually less than 10 mA/cm$^2$ in a similar condition. The 3 h oxidation time in the hydrothermal reactor is long enough. Initial current density increases exponentially with the oxidation temperature. The lower grade coal has a better activity, while in contrast, pure carbon matter is more difficult to be oxidized than coal. A further investigation of the partial oxidation mechanism of ferric ions has been made. It indicates that the oxidation between coal particles and ferric ions happens on the functional groups or aliphatic carbon attached to the core of coal. In the process of oxidation, lots of oxygen atoms from water molecules are added to the structure of coal. The resulting hydrogen atoms are released into the solution in the form of ions, which will be reduced at the cathode in electrochemical cell. Carbon dioxide comes from the thermal decomposition of the production of partial oxidation.



https://doi.org/10.1021/acsomega.1c06759
ACS Omega 2022, 7, 7865−7873

## AUTHOR INFORMATION


### Corresponding Author

**Sheng Sui** − *Institute of Fuel Cell, Shanghai Jiao Tong University, Shanghai 200240, China*; Email: ssui@sjtu.edu.cn

### Authors

**Niyi Olukayode** − *Institute of Fuel Cell, Shanghai Jiao Tong University, Shanghai 200240, China*; orcid.org/0000-0002-3957-5384

**Weijing Yang** − *State Key Laboratory of Space Power-Sources Technology, Shanghai Institute of Space Power-Sources, Shanghai 200245, China*

**Kang Xiang** − *Institute of Fuel Cell, Shanghai Jiao Tong University, Shanghai 200240, China*

**Shenrong Ye** − *Institute of Fuel Cell, Shanghai Jiao Tong University, Shanghai 200240, China*

**Zhigang Sun** − *Sinopec Ningbo Engineering Co. Ltd (SNEC), Ningbo 315103, China*

**Zhenfei Han** − *Sinopec Ningbo Engineering Co. Ltd (SNEC), Ningbo 315103, China*

Complete contact information is available at: https://pubs.acs.org/10.1021/acsomega.1c06759


### Author Contributions

N.O.: writing—review and editing and data curation. W.Y.: writing—review and editing and formal analysis. K.X.: writing—original draft, methodology, and investigation. Z.S.: formal analysis and methodology. Z.H.: resources. S.S.: conceptualization, supervision, and funding acquisition.

### Notes

The authors declare no competing financial interest.

## ACKNOWLEDGMENTS

Sui acknowledges funding from Sinopec Ningbo Engineering Co., Ltd. (SNEC) in conducting this work.

## REFERENCES


(1) Amikam, N.; Fridman-Bishop, N.; Gendel, Y. Biochar-assisted iron-mediated water electrolysis process for hydrogen production. *ACS Omega* **2020**, *5*, 31908−31917.

(2) Gielen, D.; Simbolotti, G. *Prospects for Hydrogen and Fuel Cells*; International Energy Agency Publications: Paris Cedex, France, 2005.

(3) Holladay, J. D.; Hu, J.; King, D. L.; Wang, Y. An overview of hydrogen production technologies. *Catal. Today* **2009**, *139*, 244−260.

(4) Botte, G.; Jin, X. *Hydrogen production from coal electrolysis*. In Proc. NHA Annual Hydrogen Conference, 2007, 1−4.

(5) Ju, H.; Giddey, S.; Badwal, P.; Mulder, R. J.; Gengenbach, T. R. Methanol-water co-electrolysis for sustainable hydrogen production with PtRu/C-$SnO_2$ electro-catalyst. *Ionics* **2018**, *24*, 2367−2378.

(6) Wang, M.; Wang, Z.; Gong, X.; Guo, Z. The intensification technologies to water electrolysis for hydrogen production-a review. *Renewable Sustainable Energy Rev.* **2014**, *29*, 573−588.

(7) Chen, C.; Bai, Q.; Liu, J.; Wang, Z.; Cen, K. Characteristics and anode reaction of organic wastewater-assisted coal electrolysis for hydrogen production. *Int. J. Hydrogen Energy* **2020**, *45*, 20894−20903.

(8) Take, T.; Tsurutani, K.; Umeda, M. Hydrogen production by methanol-water solution electrolysis. *J. Power Sources* **2007**, *164*, 9−16.

(9) Ju, H.; Giddey, S.; Badwal, P. S.; Mulder, R. J. Electrocatalytic conversion of ethanol in solid electrolyte cells for distributed hydrogen generation. *Electrochim. Acta* **2016**, *212*, 744−757.

(10) Ju, H.; Giddey, S.; Badwal, P. S. The role of nanosized $SnO_2$ in Pt-based electrocatalysts for hydrogen production in methanol assisted water electrolysis. *Electrochim. Acta* **2017**, *229*, 39−47.

(11) Ju, H.; Badwal, S.; Giddey, S. A comprehensive review of carbon and hydrocarbon assisted water electrolysis for hydrogen production. *Appl. Energy.* **2018**, *231*, 502−533.

(12) Chen, L.; Nakamoto, R.; Kudo, S.; Asano, S.; Hayashi, J.-I. Biochar-assisted water electrolysis. *Energy Fuels* **2019**, *33*, 11246−11252.

(13) Coughlin, R. W.; Farooque, M. Hydrogen production from coal, water, and electrons. *Nature* **1979**, *279*, 301−303.

(14) Farooque, M.; Coughlin, R. W. Anodic coal reaction lowers energy consumption of metal electrowinning. *Nature* **1979**, *280*, 666−668.

(15) Farooque, M.; Coughlin, R. W. Electrochemical gasification of coal (investigation of operating conditions and variables). *Fuel* **1979**, *58*, 705−712.

(16) Coughlin, R. W.; Farooque, M. Electrochemical gasification of coal-simultaneous production of hydrogen and carbon dioxide by a single reaction involving coal, water and electrons. *Ind. Eng. Chem. Process Des. Dev.* **1980**, *19*, 211−219.

(17) Yu, P.; Jiang, H.; Peng, R.; Ma, H.; Zheng, R.; Zhang, J. Z.; Botte, G. G. Novel Pd-Cr electrocatalyst with low Pd content for coal electrolysis for hydrogen production. *J. Power Sources* **2021**, *483*, No. 229175.

(18) Kou, K.; Zhou, W.; Chen, S.; Wang, Y.; Gao, J. Investigate the role of different inherent minerals in PEM based coal assisted water electrolysis cell. *J. Electrochem. Soc.* **2019**, *166*, F949−F955.

(19) Yin, R.; Ji, X.; Zhang, L.; Lu, S.; Cao, W.; Fan, Q. Multilayer nano Ti/$TiO_2$-Pt electrode for coal-hydrogen production. *J. Electrochem. Soc.* **2007**, *154*, 637−641.

(20) Yin, R.; Zhao, Y.; Lu, S.; Wang, H.; Cao, W.; Fan, Q. Electrocatalytic oxidation of coal on Ti-supported metal oxides coupled with liquid catalysts for $H_2$ production. *Electrochim. Acta* **2009**, *55*, 46−51.

(21) Patil, P.; De Abreu, Y.; Botte, G. G. Electrooxidation of coal slurries on different electrode materials. *J. Power Sources* **2006**, *158*, 368−377.

(22) Sathe, N.; Botte, G. G. Assessment of coal and graphite electrolysis on carbon fiber electrodes. *J. Power Sources* **2006**, *161*, 513−523.

(23) Yu, P.; Botte, G. G. Bimetallic Platinum-Iron electrocatalyst supported on carbon fibers for coal electrolysis. *J. Power Sources* **2015**, *274*, 165−169.

(24) Yu, T.; Lv, S.; Zhou, W.; Cao, W.; Fan, C. Q.; Yin, R. Catalytic effect of $K_3Fe(CN)_6$ on hydrogen production from coal electro-oxidation. *Electrochim. Acta* **2012**, *83*, 485−489.

(25) Yu, P.; Ma, J.; Zhang, R.; Zhang, Z. J.; Botte, G. Novel Pd-Co electrocatalyst supported on carbon fibers with enhanced electro-catalytic activity for coal electrolysis to produce hydrogen. *ACS Appl. Energy Mater.* **2018**, *1*, 267−272.

(26) Hesenov, A.; Meryemoglu, B.; Icten, O. Electrolysis of coal slurries to produce hydrogen gas: Effects of different factors on hydrogen yield. *Int. J. Hydrogen Energy* **2011**, *36*, 12249−12258.

(27) Jin, X.; Botte, G. G. Feasibility of hydrogen from coal electrolysis at intermediate temperatures. *J. Power Sources* **2007**, *171*, 826−834.

(28) Jin, X.; Botte, G. G. Understanding the kinetics of coal electrolysis at intermediate temperatures. *J. Power Sources* **2010**, *195*, 4935−4942.

(29) Chen, S.; Zhou, W.; Ding, Y.; Zhao, G.; Gao, J. Coal-assisted water electrolysis for hydrogen production: Evolution of carbon structure in different-rank coal. *Energy Fuels* **2021**, *35*, 3512−3520.

(30) Anthony, K. E.; Linge, H. G. Oxidation of coal slurries in acidified Ferric Sulfate. *J. Electrochem. Soc.* **1983**, *130*, 2217−2219.

(31) Dhooge, P. M.; Stilwell, D. E.; Park, S. M. Electrochemical studies of coal slurry oxidation mechanisms. *J. Electrochem. Soc.* **1982**, *129*, 1719−1724.

(32) Dhooge, P. M.; Park, S. M. Electrochemistry of coal slurries, studies on various experimental parameters affecting oxidation of coal slurries. *J. Electrochem. Soc.* **1983**, *130*, 1029−1036.

(33) Baldwin, R. P.; Jones, K. F.; Joseph, J. T.; Wong, J. L. Voltammetry and electrolysis of coal slurries and h-coal liquids. *Fuel* **1981**, *60*, 739−743.
(34) Sui, S.; Jia, J. A process for producing pure hydrogen and carbon dioxide from coal. Chinese Patent CN 201310096085.3, April 7th, 2015.
(35) Jia, J.; Sui, S.; Zhu, X.-J.; Huang, B. Effect of kinetic factors on hydrogen production by coal slurry electrolysis. *J. Fuel Chem. Technol.* **2013**, *41*, 139−143.
(36) Baker, G. G.; Sears, R. E.; Maas, D. J.; Potas, T. A.; Willson, W. G.; Farnum, S. A. Hydrothermal preparation of low-rank coal-water fuel slurries. *Energy* **1986**, *11*, 1267−1280.
(37) Thomas, G.; Chettiar, M.; Birss, V. I. Electrochemical oxidation of acidic Alberta coal slurries. *J. Appl. Electrochem.* **1990**, *20*, 941−950.
(38) Miura, K.; Mae, K.; Li, W.; Kusawa, T.; Morozumi, F.; Kumano, A. Estimation of hydrogen bond distribution in coal through the analysis of OH stretching bands in diffuse reflectance infrared spectrum measured by in-situ technique. *Energy Fuels* **2019**, *15*, 599−610.
(39) Ibarra, J. V.; Munoz, E.; Moliner, R. FTIR study of the evolution of coal structure during the coalification process. *Org. Geochem.* **1996**, *24*, 725−735.
(40) Guillen, M. D.; Iglesias, M. J.; Dominguez, A.; Blanco, C. G. Semi-quantitative FTIR analysis of a coal tar pitch and its extracts and residues in several organic solvents. *Energy Fuels* **1992**, *6*, 518−525.
(41) Sasaki, M.; Wahyudiono, Y. A.; Goto, M. Applications of hydrothermal electrolysis for conversion of 1-butanol in wastewater for treatment. *Fuel Process. Technol.* **2010**, *91*, 1125−1132.
(42) Hauch, A.; Ebbesen, S. D.; Jensen, S. H.; Mogensen, M. Highly efficient high temperature electrolysis. *J. Mater. Chem.* **2008**, *18*, 2331−2340.
(43) Ebbesen, S. D.; Jensen, S. H.; Hauch, A.; Mogensen, M. B. High Temperature Electrolysis in Alkaline Cells, Solid Proton Conducting Cells, and Solid Oxide Cells. *Chem. Rev.* **2014**, *114*, 10697−10734.
(44) Barbir, F. Fuel Cell Electrochemistry. In *PEM Fuel Cells*, 2nd ed.; Academic Press: Boston, 2013.
(45) Grassinger, H. What is the difference between current density and exchange current density? Quora. May 16th, 2020. Accessed: December 26th, 2021. https://www.quora.com/What-is-the-difference-between-current-density-and-exchange-current-density
(46) Gennero de Chialvo, M. R.; Chialvo, A. C. Exchange current density, electrocatalytic activity and volcano curve for the hydrogen electrode reaction: theoretical analysis. *Curr. Top. Electrochem.* **2012**, *17*, 41−52.
(47) Hasoi, T.; Yonekura, T.; Sunada, K.; Sasaki, K. Exchange Current density of SOFC electrodes: theoretical relations and partial pressure dependencies rate-determined by electrochemical reactions. *J. Electrochem. Soc.* **2015**, *162*, F136.
(48) Karim, K.; Esrafili, M. D.; Ehsani, A. Graphene and Anticorrosive Properties. In Graphene Surfaces-Particles and Catalsts, 1st ed. *Interface Sci. Technol* **2019**, *27*, 303−337.
(49) Ge, L.; Gong, X.; Wang, Z.; Zhao, L.; Wang, Y.; Wang, M. Insight of anode reaction for CWS (coal water slurry) electrolysis for hydrogen production. *Energy* **2016**, *96*, 372−382.


https://doi.org/10.1021/acsomega.1c06759
*ACS Omega* 2022, 7, 7865−7873